JOURNAL OF MATERIALS SCIENCE 33 (1998) 743–748

Preparation and study of $Ca_{1-x}Mg_x(PO_3)_2$ glassy and crystalline phases

P. PROKŮPKOVÁ, P. MOŠNER, L. KOUDELKA, M. VLČEK
University of Pardubice, 53210 Pardubice, Czech Republic

The structure of $Ca_{1-x}Mg_x(PO_3)_2$ crystalline and glassy samples was investigated in the whole concentration region of $x = 0$–1.0. From X-ray diffraction data it was found that, in the crystalline samples, solid solutions are formed for $x < 0.3$ on the calcium-side of the system, with the structure of β-$Ca(PO_3)_2$, and for $x > 0.6$ on its magnesium-side, with the structure of $Mg_2P_4O_{12}$. Similar results were obtained from the study of their infrared and Raman spectra. In the glassy state, homogeneous glasses were formed within the whole concentration region. The values of their transformation temperatures, T_g, and crystallization temperature, T_c, change slightly with the composition and lie within the region of $T_g = 529$–544 °C and $T_c = 631$–677 °C. © *1998 Chapman & Hall*

1. Introduction

Calcium phosphates belong to materials studied for their application in medicine as biomaterials with unique properties [1] in both the crystalline and glassy phases. Hydroxyapatite and calcium metaphosphate are the most interesting compounds which have been studied in recent years [2, 3] for this purpose.

The metaphosphates have an ability to form a glassy state during rapid cooling of their melt. The substitution of calcium in the metaphosphates by magnesium with a higher electronegativity and a smaller atomic volume, has not yet been studied properly. Crystalline tetraphosphates of calcium and magnesium differ in their structure [4, 5], the former forming four-member rings, and formula often being written as $Mg_2P_4O_{12}$ while the latter forms phosphate chains and the formula $[Ca_2(PO_3)_4]_x$ is used for the description of its structure. We have studied how the structure of the mixed phases $Ca_{1-x}Mg_x(PO_3)_2$ is reflected in some properties of these materials both in the crystalline and glassy states. The effect of their composition on their structure was evaluated mainly through analysis of their X-ray diffraction patterns and Raman and infrared spectra.

2. Experimental procedure

The samples of the system $Ca_{1-x}Mg_x(PO_3)_2$ were prepared with the compositions of $x = 0$, 0.2, 0.4, 0.5, 0.6, 0.8 and 1.0. The preparation of samples started from carbonates of calcium and magnesium and the phosphoric acid solution containing 85% pure H_3PO_4. The starting compounds were mixed in the stoichiometric ratio corresponding to the following reaction

$$(1-x)CaCO_3 + xMgCO_3 + 2H_3PO_4 \rightarrow Ca_{1-x}Mg_x(H_2PO_4)_2 + CO_2 + H_2O \qquad (1)$$

Phosphoric acid was added slowly to the starting suspension of carbonates premixed with a small amount of water. The obtained suspension was then dried at 60 °C.

The dry product was slowly heated to 600 °C and this temperature was maintained for 2 h. The obtained material was disintegrated in the vibrational mill and melted at 1250 °C for 20 min; then the melt was cooled rapidly either by pouring into the water or onto a steel sheet.

The process of dehydration of the starting material was studied by thermogravimetry (TG) and differential thermal analysis (DTA) on the Derivatograph (Budapest) equipment in air in the temperature region 20–600 °C at a heating rate of 4 °C min^{-1}. Crystallization of the glassy samples was studied on Perkin-Elmer DTA equipment, model 1700, in the temperature region 20–1000 °C at a scan rate 15 °C min^{-1}. The glassy samples used for the investigation of thermal properties were disintegrated in the vibrational mill.

Infrared spectra were obtained using a Perkin Elmer model 684 infrared spectrometer, with the powder samples dispersed in nujol mulls. Raman spectra were measured on a Fourier transform–infrared (FT–IR) spectrometer, Bruker model IFS 55, with the Raman attachment, FRA 106, at room temperature under excitation with Nd:YAG laser radiation using a slit width of 4 cm^{-1} with the power at the sample of 400 mW. The glassy samples were in the bulk form; crystalline samples were studied both in powder and bulk form.

3. Results and discussion

3.1. Thermal analysis

In Fig. 1, as an example, TG and DTA curves are presented of the decomposition of a starting mixture

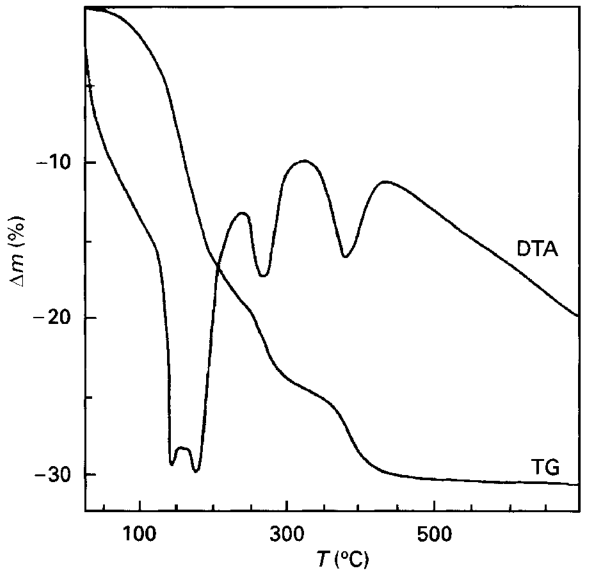

Figure 1 Thermal analysis (TG + DTA) of starting products during the formation of $Ca_{0.5}Mg_{0.5}(PO_3)_2$ sample.

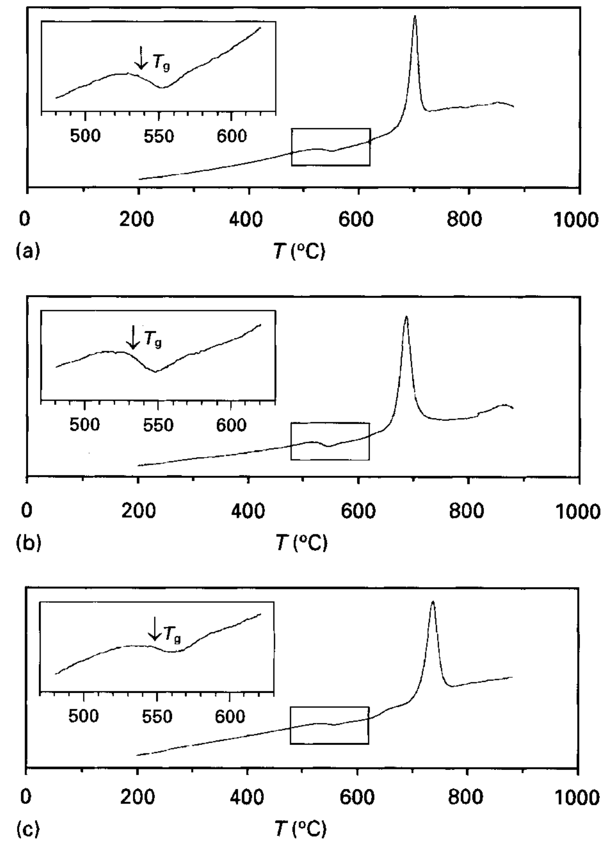

Figure 2 Differential thermal analysis of the $Ca_{1-x}Mg_x(PO_3)_2$ glasses: (a) $Ca_{0.5}Mg_{0.5}(PO_3)_2$, (b) $Ca(PO_3)_2$, (c) $Mg(PO_3)_2$.

TABLE I The values of the transformation temperature, T_g, and the crystallization temperature, T_c of the $Ca_{1-x}Mg_x(PO_3)_2$ glasses obtained by cooling in water

	x						
	0	0.2	0.4	0.5	0.6	0.8	1
T_g (°C)	533	535	537	533	535	540	548
T_c (°C)	631	652	658	663	671	675	677

of dihydrogenphosphate $Ca_{0.5}Mg_{0.5}(H_2PO_4)_2 \cdot xH_2O$ on heating to 600 °C. The identification of the products obtained after the heating was carried out by X-ray diffraction analysis.

The decomposition of $Mg(H_2PO_4)_2 \cdot xH_2O$ proceeds in three successive steps. In the first, the weight loss corresponds to the escape of about 2 mol water crystallization and the formation of anhydrous $Ca_{0.5}Mg_{0.5}(H_2PO_4)_2$. The following two steps correspond to the process of conversion of this compound into magnesium metaphosphate, $Mg_2P_4O_{12}$. Some authors suppose the formation of dihydrogen pyrophosphate $MgH_2P_2O_7$ in the first step of the decomposition of metaphosphates.

The decomposition of $Ca(H_2PO_4)_2 \cdot xH_2O$ is similar to the previous one, but the decomposition steps are not so clearly separated, but proceed more continuously one after the other. The weight loss in the first step also corresponds to slightly less than 2 mol water crystallization, and the decomposition of $Ca(H_2PO_4)_2$ into the calcium metaphosphate $[Ca_2P_4O_{12}]_n$ proceeds also in two steps. A similar course of decomposition was observed also for a sample of mixed phosphate $Ca_{0.5}Mg_{0.5}(H_2PO_4)_2 \cdot xH_2O$ (Fig. 1). The first decomposition step is accompanied by two close peaks on the DTA curve, and thus it seems that the first decomposition (the loss of water crystallization) proceeds in two substeps.

Differential thermal analysis of the $Ca_{1-x}Mg_x(PO_3)_2$ glassy samples showed two distinct enthalpic effects (see Fig. 2), the first one is the glass transformation effect, T_g, and the second one belongs to the crystallization, T_c, which starts about 200 °C above the transformation temperature. The T_g value was taken as the temperature corresponding to the inflexion point in the decreasing part of the DTA curve, the T_c value corresponds to the onset temperature of the crystallization peak. There are slight changes in the values of T_g and T_c with composition of the samples and with the rate of cooling of the melt. The obtained values of T_g and T_c (onset) are given in Table I. The value of T_c increases slightly with increasing content of magnesium from 631–677 °C for the samples cooled in water. The differences in both values for the glasses prepared by cooling in water or on a steel sheet, are small, and no regularities in the differences between both ways of cooling were observed. The method of cooling the melt in water gave samples with more reproducible thermal properties.

3.2. X-ray diffraction

The crystallization of the glassy samples leads to the formation of crystalline phases, the structure of which, according to the X-ray diffraction analysis, is the same as the structure of the crystalline material obtained by the heat treatment of the starting mixture to 600 °C. The obtained values of interplanar spacings d_{hkl} are

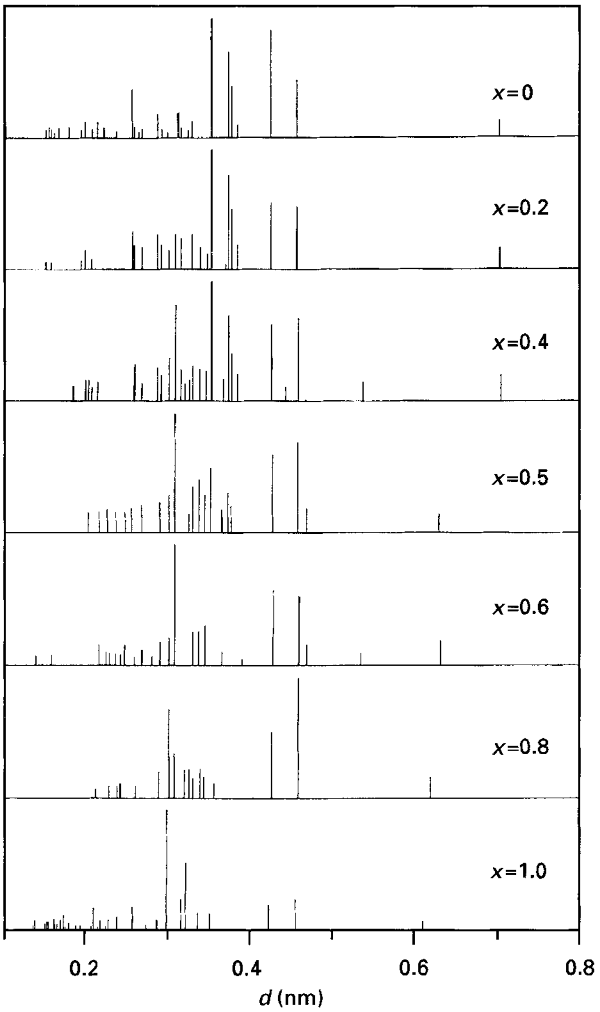

Figure 3 X-ray diffraction patterns of crystalline $Ca_{1-x}Mg_x(PO_3)_2$ samples, obtained by heating the starting mixture to 600 °C.

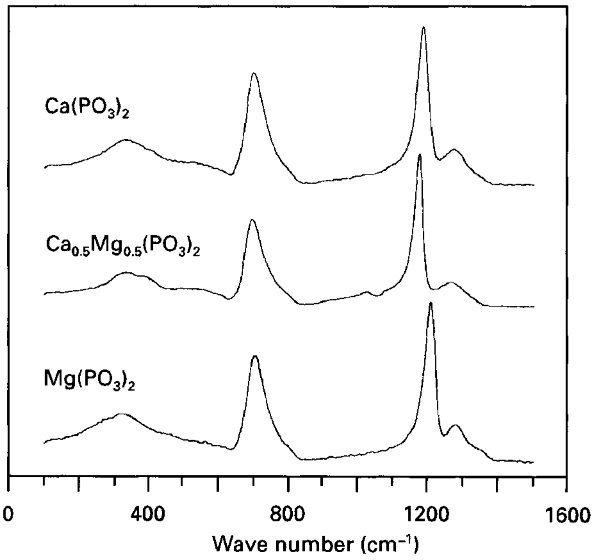

Figure 4 Raman spectra of $Ca_{1-x}Mg_x(PO_3)_2$ glasses.

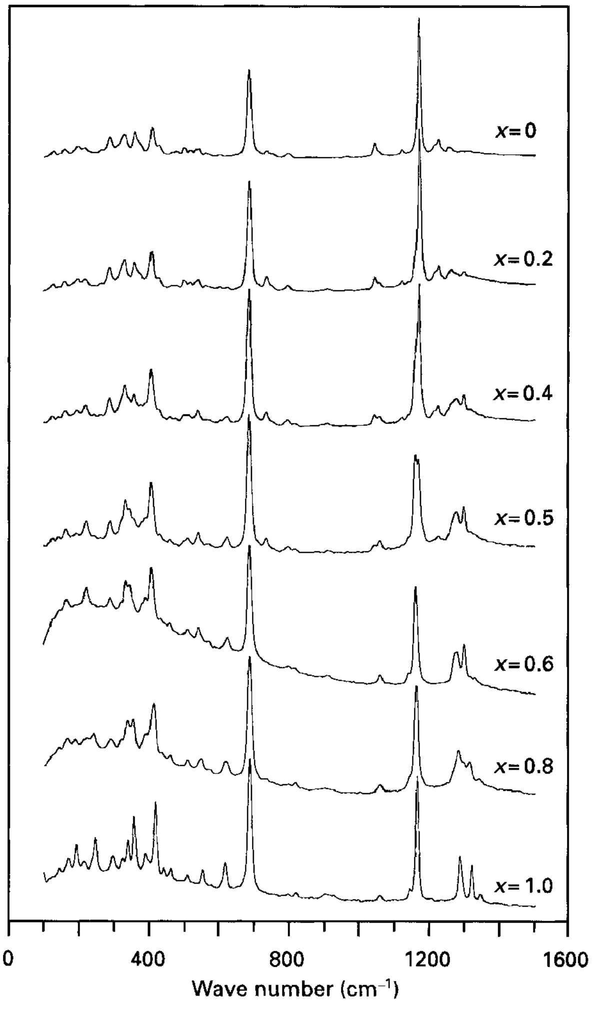

Figure 5 Raman spectra of crystalline $Ca_{1-x}Mg_x(PO_3)_2$ samples.

given in Fig. 3. The X-ray diffraction patterns agree well with the literature data on the corresponding crystalline metaphosphates [6]; on the calcium-side with the β-$Ca(PO_3)_2$ structure and on the magnesium-side with the $Mg_2P_4O_{12}$ structure, respectively. The structure of the first one is composed of linear chains, while the other forms tetraphosphate rings of $P_4O_{12}^{4-}$. On the X-ray diffraction patterns (Fig. 3) no other lines were found than those of the compounds β-$Ca(PO_3)_2$ and $Mg_2P_4O_{12}$, i.e. there is no new compound formed within this system. On both sides of the $Ca_{1-x}Mg_x(PO_3)_2$ system, were found regions of solid solution formation. On the calcium side it reaches to about $x \sim 0.3$ and on the magnesium side up to $x \sim 0.6$, i.e. about 30% of the calcium can be replaced by magnesium in the crystalline phase, whereas about 40% Mg can be replaced by calcium in the crystalline $Mg_2P_4O_{12}$ without a change in their structure. The differences in the structure of the crystalline phases are reflected also in their vibrational spectra.

3.3. Raman spectra

Figs 4 and 5 show Raman spectra of glassy and crystalline $Ca_{1-x}Mg_x(PO_3)_2$ samples, respectively. A similar character of infrared and Raman spectra of both crystalline and glassy phases (especially the same positions of strong vibrational bands in their Raman spectra) also gives evidence for a quasi-characteristic type of vibrations of their basic structural groups.

According to Poletaev [7, 8], the vibrational spectra of crystalline metaphosphates can be ascribed to the vibrations of the groups of P–O–P and $=PO_2$ which are included in their structure consisting of chains or rings. Therefore, in their vibrational spectra there are distinct intervals of frequencies which can be assigned to the stretching frequencies of $\nu_{as}(PO_2) =$ 1180–1350 cm^{-1}, $\nu_s(PO_2) =$ 1080–1180 cm^{-1}, ν_{as}(POP) = 850–1080 cm^{-1} and ν_s(POP) = 660–820 cm^{-1}.

The Raman spectra of $Ca_{1-x}Mg_x(PO_3)_2$ glasses (Fig. 4) show two strong bands assigned to vibrations of the metaphosphate chain network. The symmetric stretching vibration of P–O–P bonds occurs at about 700–710 cm^{-1} and the symmetric stretching vibration of PO_2 groups lies between 1180 and 1215 cm^{-1}. The position of the second band shifts more to higher frequencies with the replacement of calcium by magnesium. The differences in the band positions can be explained partly as due to the differences in the masses of the cations Ca^{2+} and Mg^{2+}, but more due to a stronger coupling of Mg^{2+} to the anionic polyphosphate chain.

Raman spectra of crystalline $Ca_{1-x}Mg_x(PO_3)_2$ phases (Fig. 5) reveal more pronounced differences than those of the corresponding glasses. The spectral region between 1200 and 1350 cm^{-1} contains the bands corresponding to the asymmetric stretching vibrations of PO_2 groups in the metaphosphate network, while the region between 1050 and 1200 cm^{-1} contains the bands assigned to symmetric stretching vibrations of PO_2 groups.

In the region between 850 and 1050 cm^{-1}, there are the bands corresponding to asymmetric stretching vibrations of P–O–P bonds, whereas between 600 and 850 cm^{-1} there are the bands caused by symmetrical stretching vibrations of the P–O–P linkages.

TABLE II Raman spectra of crystalline $Ca_{1-x}Mg_x(PO_3)_2$ samples

$Ca(PO_3)_2$ (cm^{-1})	$Ca_{0.5}Mg_{0.5}(PO_3)_2$ (cm^{-1})	$Mg(PO_3)_2$ (cm^{-1})	Assignment
		1347 vw	
	1300 w	1322 w	$\nu_{as}(PO_2)$
1257 vw	1279 w	1289 w	
1228 vw	1230 vw		
1173 vs	1172 s,sh		
	1162 s	1167 vs	$\nu_s(PO_2)$
1124 vw			
	1063 vw	1062 sh	
1047 vw			ν_{as}(POP)
		905 vw	
798 vw	798 vw		
688 s	688 vs	689 vs	ν_s(POP)
	625 vw	619 w	
543 vw	542 vw	554 w	
501 vw	511 vw	509 vw	
409 w	408 m	417 s	
360 vw	358 sh	357 s	
331 vw	333 w	339 m	
		324 w	PO_2 bend
289 vw	290 w	298 w	POP bend
	222 w	215 w	
199 vw		194 m	
159 vw	164 vw	171 w	
129 vw	126 vw		
		101 w	

Finally, the region 100–600 cm^{-1} contains the bands caused by deformation vibrations of the metaphosphate chain skeleton. The summary of the positions of vibrational bands for three representative samples is given in Table II.

The differences in the peak positions of the main bands at ~ 700 and ~ 1180 cm^{-1} between the Raman spectra of the $Ca_{1-x}Mg_x(PO_3)_2$ crystalline phases are smaller than at the corresponding glasses, but in the region 1200–1350 cm^{-1} the changes in the position of the bands due to asymmetric stretching of PO_2 groups are substantial. The bands of 1278 and 1300 cm^{-1} can be seen in the spectra within the compositional region of $x = 0.5$–1.0 in the magnesium rich samples, the sample with $x = 0.4$ has the features of both magnesium and calcium metaphosphate. At the calcium rich samples there are small bands of 1228 and 1257 cm^{-1}.

The observed differences in this high-frequency region of the vibrational spectra may be due to the differences in the interaction of the anion lattice with the cation–oxygen vibrations influenced by a stronger interaction of covalent Mg–O bonds than at the more ionic Ca–O bonds. Such interactions are manifested most of all in the region of deformational vibrations under 650 cm^{-1}.

3.4. Infrared spectra

Figs 6 and 7 show infrared spectra of glassy and crystalline $Ca_{1-x}Mg_x(PO_3)_2$ phases. The infrared spectra of the $Ca_{1-x}Mg_x(PO_3)_2$ glasses are very similar each to other, having strong bands at 1300 cm^{-1} (ν_{as} PO_2) 1080 and 1020 cm^{-1} (ν_s PO_2) and 920 and 1010 cm^{-1} (ν_{as} P–O–P). Two weaker bands at 720 and 800 cm^{-1} can be ascribed to the symmetric vibrations

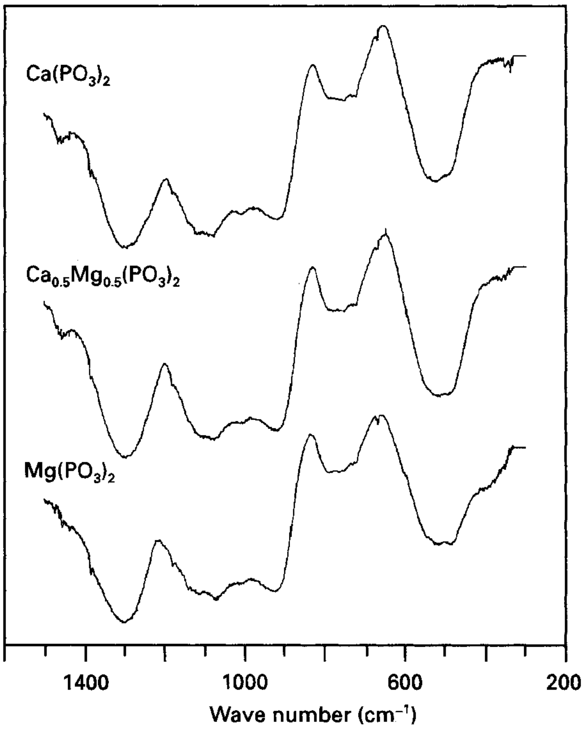

Figure 6 Infrared spectra of $Ca_{1-x}Mg_x(PO_3)_2$ glasses.

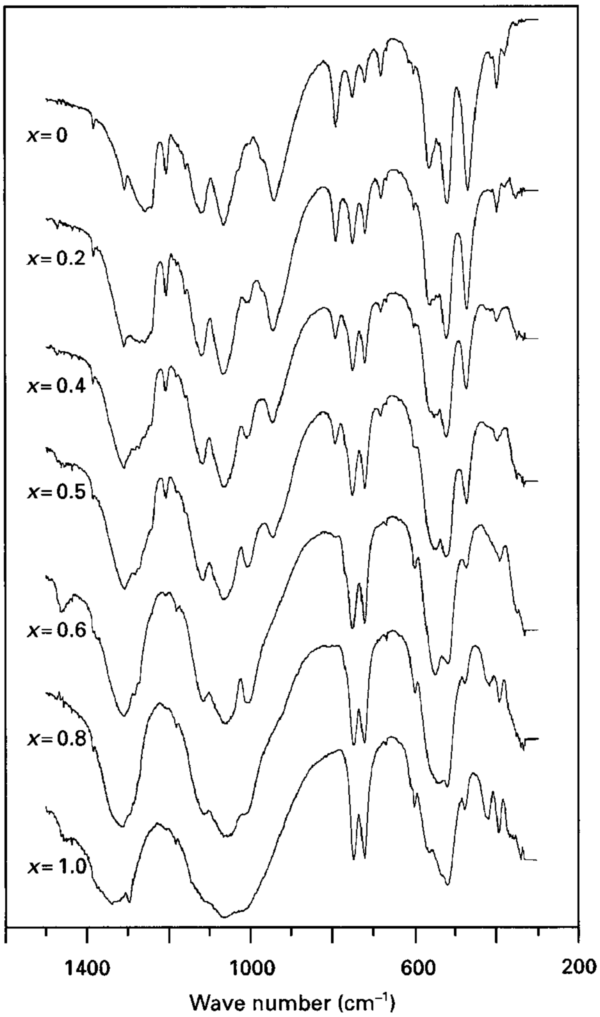

Figure 7 Infrared spectra of crystalline $Ca_{1-x}Mg_x(PO_3)_2$ samples.

of P–O–P bonds and the bands between 490 and 530 cm^{-1} to bending vibrations of the structural network.

Infrared spectra of crystalline phases of $Ca_{1-x}Mg_x(PO_3)_2$ having $x = 0.6$–1.0 retain mostly the structure of pure crystalline $Mg_2P_4O_{12}$. The centre of the main band of $\nu_{as}(PO_2)$ shifts a little to lower values with increasing x value. In the calcium-rich samples, there are four bands in the region of ν_s(POP), whereas only two bands are present in the spectra of calcium-rich samples. Also the region of 900–1300 cm^{-1} at the calcium-rich samples has more distinct vibrational bands than at the samples on the magnesium-rich region, where there is a broad band between 900 and 1150 cm^{-1}. The summary of the positions of vibrational bands for three representative crystalline samples is given in Table III.

On the opposite side, the infrared spectra of $Ca_{1-x}Mg_x(PO_3)_2$ glasses do not reveal any substantial differences through the whole spectral region of 200–1500 cm^{-1}. This provides evidence for the same structure of all the glassy samples within the whole compositional region. Their structure is composed of $-(PO_2)-O-(PO_2)-O-(PO_2)-$ chains, whereas in the crystalline phase magnesium metaphosphate has a ring-like structure [4].

TABLE III Infrared spectra of crystalline $Ca_{1-x}Mg_x(PO_3)_2$ samples

$Ca(PO_3)_{12}$ (cm^{-1})	$Ca_{0.5}Mg_{0.5}(PO_3)_2$ (cm^{-1})	$Mg(PO_3)_2$ (cm^{-1})	Assignment
1386 m			
		1338 vs	$\nu_{as}(PO_2)$
1311 s	1308 vs	1297 sh	
1258 vs			
1208 s	1207 m		
1160 sh	1115 vs		
1123 vs			$\nu_s(PO_2)$
1069 vs	1061 vs	1061 vs	ν_{as}(POP)
	1009 s		
942 vs	945 s		
792 m	763 w		
751 w	750 m	747 s	ν_s(POP)
722 w	720 m	720 s	
682 w			
566 s	553 s	599 w	
521 vs	522 s	520 s	
471 s	475 m	478 sh	PO_2 bend
		419 m	POP bend
401 w	401 w	394 m	
		339 s	

4. Conclusion

The structure of $Ca_{1-x}Mg_x(PO_3)_2$ crystalline and glassy samples was investigated in the whole concentration region of $x = 0$–1.0. From the X-ray diffraction study of crystalline samples the regions of formation of solid solutions was estimated to be $x < 0.3$ on the calcium side of the system having the structure of β-$Ca(PO_3)_2$ and $x > 0.6$ on its magnesium side having the structure of $Mg_2P_4O_{12}$. Analysis of their infrared and Raman spectra gave similar conclusions. There are very small differences in the Raman and infrared spectra of the $Ca_{1-x}Mg_x(PO_3)_2$ glasses, which are homogeneous within the whole concentration region $x = 0$–1.0. The differences in the Raman and infrared spectra of crystalline samples are due to their different symmetries of the crystalline phases caused by a greater tendency of magnesium metaphosphate to form rings of P_4O_{12} in their structure, whereas calcium metaphosphate forms linear chains. In the glassy state of $Ca_{1-x}Mg_x(PO_3)_2$ samples the chains are formed within the whole concentration region of $x = 0$–1.0

Acknowledgement

This research was carried out with the financial support from the Czech Grant Agency (Project Code 104/94/0801).

References

1. M. JARCHO, *Clin. Orthop. Rel. Res.* **157** (1981) 259.
2. A. BERTOLUZZA, S. CACCIARI, A. TINTI and M. VASINA, *J. Mater. Sci. Mater. Med.* **6** (1995) 76.
3. A. BERTOLUZZA, in "*Spectroscopy of Biological Molecules*", edited by C. Sandorfy and T. Theopanides (Reidel, 1984) pp. 191–211.

4. M. SCHNEIDER, K-H. JOST and P. LEIBNITZ, *Z. Anorg. Allg. Chem.* **527** (1985) 99.
5. A. G. NORD and K. B. LINDBERG, *Acta Chem. Scand.* **A 29** (1) (1975) 1.
6. "X-ray diffraction data cards", American Society for Testing and Materials, Philadelphia, 1968, cards 17-500 and 18–782.
7. E. V. POLETAEV, *Izv. Akad. Nauk Kaz. SSR Ser. Khim.* (1) (1968) 42.
8. *Idem., ibid.* (5) (1968) 1.

Received 23 July 1996
and accepted 22 August 1997